

OPTIMIZATION ASSISTED AUTOREGRESSIVE METHOD WITH DEEP CONVOLUTIONAL NEURAL NETWORK-BASED ENTROPY FILTER FOR IMAGE DEMOSAICING

C. Anitha Mary and A. Boyed Wesley

Department of Computer Science, Nesamony Memorial Christian College, India

Abstract

The natural scenes are captured by digital cameras that adopt a single charged-coupled device (CCD) or Complementary Metal Oxide Semiconductor (CMOS) sensor with a Color Filter Array (CFA). To reconstruct a full color image from the mosaiced CFA image, the missing components of color are recovered by a technique called color demosaicing. This research work introduces Deep Convolution Neural Network (DCNN)-based optimization assisted autoregressive method for image demosaicing. Here, the proposed optimization algorithm, termed Adaptive Autoregressive Water Wave Optimization algorithm (Adaptive Autoregressive-WWO), that is formed by combining Conditional autoregressive value at risk (CAViaR) model and Water Wave Optimization algorithm (WWO). Fusion process is carried out for residual images to generate the final demosaiced image based on entropy measure. Here, the output generated from DCNN is the first residual image. The LPA-ICI filter utilizes the optimization algorithm that generated second order polynomial coefficients to produce the second residual output image. Moreover, this proposed method is evaluated for its performance using metrics, such as Peak signal-to-noise ratio (PSNR) and Second Derivative like Measurement (SDME) and attained the highest PSNR values of 40.379dB and highest SDME values of 50.675dB.

Keywords:

Imagedemosaicing, Local Polynomial Approximation and Intersection of Confidence Interval Filter, Entropy, Fusion Process, Deep Convolution Neural Network

1. INTRODUCTION

Demosaicing problems are the important issues for color artifacts. These artifacts are found in the edge regions and texture regions. The classical image restoration issues, like denoising, Super Resolution (SR), and demosaicing must be solved for proper clear image output. But the attention of solving these problems together is a challenge among researchers. The sequential methods of solving these issues increased complexity and resulted in the error formation. The complexity increment of the solution depends on both memory and speed [5]. The major artifacts of the color images, like denoising and demosaicing treated independently has many disadvantages when compared with treating these artifacts together.

The first stage is the amplification, while amplifying the noise, the image's edge structure is preserved, and this improvisation is done by tuning the coefficients of filter leading to the improvement in image quality. The second stage is the estimation of the pixel components that are missing. These missing pixels incorporate the sensor's noise characteristics. At last, the complexity in computation is reduced by demosaicing-denoising algorithm that led to the better artifact treating performance simultaneously [6]. Directional filtering is one of the important

filtering methods for the demosaicing process that tend to high quality image [7].

The Bayer color filter [7] array was invented in the year 1976. In this filter, half the array is covered by green pixels in a quincunx lattice, whereas the blue and red pixel locations are uniformly distributed to each two pixels [11]. Many demosaicing algorithms have been developed, and in 2004, the algorithm named Malvar–He–Cutler (MHC) [12] for Red, Green and Blue (RGB) bands demosaicing was used by Mast camera (Mastcam) images [10]. Small pitch pixels of images have low-noise and weight and hence they are weaker and not clear. To solve this issue, an end-to-end learning-based color reconstruction technique for used by grounding the deep neural network on the known physical properties of the color acquisition process. To reduce the noise issue, a sensor named Quanta Image Sensor (QIS) is used [13]. For efficiency improvement, data-driven local filtering approach is used for Denoising and demosaicing together. This model is trained on a large scale of ground truth data to reduce the regularities found in natural images optimally by deep learning [8]. The CNNs are very effective in both low-level vision problem and high-level vision problem. The deep residual learning network is successfully applied to image restoration and image recognition applications with a very deep network architecture. The demosaicing issues formulated as a deep residual learning procedure [9].

This research promotes an effective model for image demosaicing using proposed Adaptive Autoregressive WWO. Here, first the input image is filtered by LPA-ICI filter, where filter coefficients are generated. This filter coefficients are generated by proposed Adaptive Autoregressive-WWO, that is combined by CAViaR model and WWO. Similarly, the same input image is fed to DCNN. Finally, the residual image obtained from both the methods are combined by the entropy measure to form demosaiced image.

The key contribution of this work is given below:

- Introduced Adaptive Autoregressive-WWO-based LPA-ICI filter + DCNN: The successful model for image demosaicing is proposed using Adaptive Autoregressive-WWO-based LPA-ICI filter +DCNN.
- The filter coefficients are generated to enhance the image clarity. The LPA-ICI filter is trained using newly developed optimization assisted autoregressive technique, which is the combination of CAViaR [18] model and WWO [19].

The rest of the paper has the following arrangements: Section 2 illustrates the literature survey of techniques corresponding to image demosaicing along with its merits and issues. Section 3 shows the proposed strategy for image demosaicing, and section 4 depicts the results. Finally, the research papers are concluded in section 5.

2. MOTIVATION

The image sensor that generated images from the digital camera is degraded by the noise issues. But the CFA sensor in the digital camera is processed for clear image by reducing this noise issues. This processing technique known as demosaicing is presented in this paper that produced a clear demosaiced image. This section elucidates the literature reviews related to image demosaicing that tend the researchers to model the best solution for image demosaicing.

2.1 LITERATURE REVIEW

The priorly devised image demosaicing methodologies are described with its advantages and issues. Xing, and Egiazarian [1] proposed a ResidualSwin Transformer-based network (RSTCANet) for image demosaicing. RSTCANet arranged many residual Swin Transformer Channel Attention blocks (RSTCAB), that extracted image features, and this arranged channel attention to nearby Swin Transformer (ST) blocks. RSTCANet was generated much less color artifacts in the resulting images when compared with state-of-the-art performance on image demosaicing but failed to extend the RSTCANet to other image restoration tasks, such as image denoising and super-resolution. To rectify the issues in [1], Park et al. [2] presented re-interpolation process by Singular Value Decomposition (SVD) for an unknown demosaicing method. Initially, based on Bayer pattern, the image's green channel was decomposed to four sub-images. Then, SVD was performed to each small block of sub-image. The statistical model for feature extraction was not required in this method, as prediction residue was more accurate than conventional method. However, this method had a drawback to localize tampered regions in the image. The drawback in [2] was solved by Pistellato et al. [3] who proposed CNN-based model that demosaiced directly raw camera image to a single per-pixel Stokes vector. It's a two-fold type, first, a network architecture was proposed by the arrangement of Mosaiced Convolutions with local arrangement of different filters. Next, a consumer liquid crystal display (LCD) screen was employed to acquire training data. This is invariant using external lighting conditions and monitor gamma. This method was not considered with kernel shapes to increase the repeated orientation pattern combinations, wherein Luo and Wang [4] proposed Generative Adversarial Network (GAN) to generate high-quality color images. Data preparation phase was not needed in this method as it reduced computational complexity. GAN generator was designed by U-net that generated demosaicing images. This improved the discriminant ability of the network and the combination of neural network and traditional demosaicing algorithms was not tested.

2.2 CHALLENGES

The issues faced by priorly devised image demosaicing methodologies are described below.

- Existing demosaicing methods can be categorized in two methods, named learning-based methods and model-based methods. Based on both methods, there are still color artifacts in their resulting images for high frequency regions. For this, the bigger model size is considered for removing

artifacts. However, the challenge remains in choosing the model size based on depth of network with less cost [1].

- Re-interpolation process is required for demosaicing pattern-based tampering localization algorithms and to localize tampered regions, the prediction residue between re-interpolated image and the given image is commonly used. However, the prediction residue is not acceptable as interpolation kernel for demosaicing cannot be known, that declines the localization performance [2].
- The learning-based joint demosaicing and denoising algorithm in [13] gives better performance for low-light color imaging and preserves the construction quality of image whereas, this technique still has a challenge on concentrating towards network compressing capacity along the preservation of image.
- The correlation among various color channels rejects traditional interpolation-based methods, that resulted in unsmooth images. Moreover, at high-frequency areas, the interpolation-based algorithms still have some problems for image demosaicing.

3. PROPOSED ADAPTIVE AUTOREGRESSIVE WWO FOR IMAGE DEMOSAICING

The image sensor is utilized by many digital cameras in the electronics field. This sensor posed CFA for capturing color images and recorded the color components like RGB in each pixel location. This generated image is called as mosaiced image, which is the reverse image formed from the method of demosaicing.

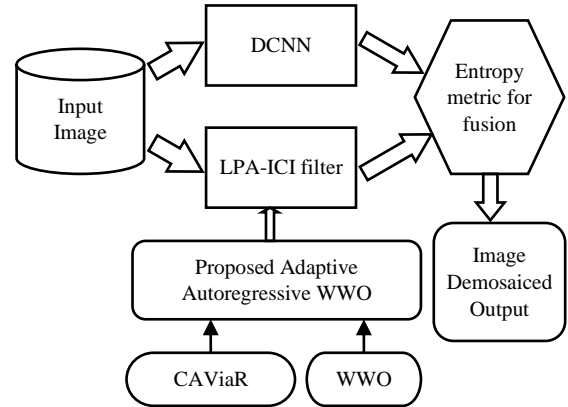


Fig.1. Structure of image demosaicing using proposed Adaptive Autoregressive WWO-based LPA-ICI model

The aim of this method is to design CNN-based entropy filter for image demosaicing. This paper induced optimization algorithm to generate LPA-ICI filter for filter coefficients. First, the input image is fed to the LPA-ICI filter for the process of filtering. Here, by proposed Adaptive Autoregressive WWO, the second-order polynomial interpolation-filter coefficients [17] are generated in this filter. CAViaR model [18] and WWO [19] are interpolated to form this proposed Adaptive Autoregressive WWO, that generated the filter coefficients. Thus, the filter output is generated by the proposed Adaptive Autoregressive-WWO-based LPA-ICI model. Simultaneously, the same input image is fed into DCNN and from this, the residual image is obtained [20]. At last, both results of Autoregressive-WWO-based LPA-ICI

model and DCNN are combined by the entropy metric to generate the final demosaiced output. The Fig.1 shows the Structure of proposed Adaptive Autoregressive WWO-based LPA-ICI model for image demosaicing.

3.1 IMAGE ACQUISITION

Initially, the image dataset is considered as H with G input image. This dataset is expressed as,

$$H = \{G_1, G_2, \dots, G_i, \dots, G_j\} ; 1 \leq i \leq j \quad (1)$$

where, j is the total number of images, G_i denotes i^{th} image, and G_j denotes total number of images. Here, the input images G_i are fed for demosaicing of the image to proposed Adaptive Autoregressive-WWO-based LPA-ICI and DCNN.

3.2 DCNN BASED IMAGEDEMOAICING

The input image G_i is given as the input to DCNN [16], here the DCNN is chosen to learn the discriminative denoisers by considering performance, speed, and color image before modelling. The DCNN is used for obtaining clear and clean image that comprises nineteen layers. Here, the yellow color indicates convolution layer and blue color indicates rectified linear activation unit (ReLU) as shown in Fig.2. Here, the DCNN output is denoted as S_1 .

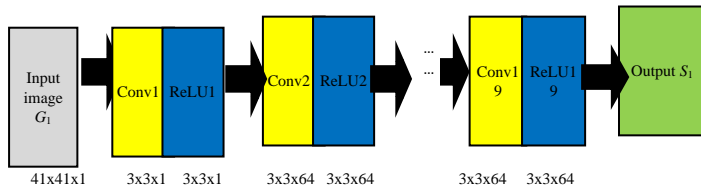


Fig.2. DCNN model for image demosaicing

3.3 LPA-ICI ALGORITHM FOR COLOR FILTER ARRAY INTERPOLATION

This section consists of three steps, like initialization, interpolation and filtering. The directional differences of the color are generated to find the degraded noise. This noise is filtered using LPA-ICI on each input image G_i and the missing color values are estimated.

• **Initialization:**

First, the directional estimates, such as vertical and horizontal estimates of green channel at each point $(p,q) \in Q$ is determined by Hamilton–Adams algorithm. Here, the interpolation of green G at red R positions that is $(p,q) \in Q_R$ is performed. The directional difference is calculated as,

$$\tilde{\Delta}_{g,r}^h(p,q) = \Delta_{g,r}(p,q) + \varepsilon_{g,r}^h(p,q) \quad (2)$$

$$\tilde{\Delta}_{g,r}^v(p,q) = \Delta_{g,r}(p,q) + \varepsilon_{g,r}^v(p,q) \quad (3)$$

where, $\varepsilon_h(i,j)$ and $\varepsilon_v(i,j)$ are random noise demosaiced, $\Delta_{g,r}(p,q)$ is the difference between G and R . Also, the same process is followed in the blue channel to calculate the directional differences, such as $\tilde{\Delta}_{g,b}^h(p,q)$ and $\tilde{\Delta}_{g,b}^v(p,q)$.

• **LPA-ICI filtering:** The LPA-ICI filtering is used for estimating all kinds of noise. The input noisy data for

filtering is given as, $r(p,q)$ that indicates noisy estimates, $t(p,q)$ indicates noise and $s(p,q)$ represents the true signals. The input data is filtered by assuming input noisy data that is formulated as,

$$r(p,q) = s(p,q) + t(p,q) \quad (4)$$

• **G-color Interpolation:** The G -color Interpolation is computed using the expression given below:

$$\hat{G}(p,q) = R(p,q) + \hat{\Delta}_{gr}(p,q) ; (p,q) \in Q_R \quad (5)$$

$$\hat{G}(p,q) = B(p,q) + \hat{\Delta}_{gb}(p,q) ; (p,q) \in Q_B \quad (6)$$

$\hat{\Delta}_{gr}$ illustrates G-R estimate and $\hat{\Delta}_{gb}$ shows G-B estimate.

• **Interpolation of R/B Color at B/R Positions:** A special shift-invariant interpolation filter is utilized for this process that provides the estimates using standard convolution. This filter is devised considering the sub-sampled grid of LPA that is related to channel by symmetrical window function.

• **Interpolation of R/B Color at G Positions:** The simplest zero-order interpolation kernel is utilized for this process. From this, using proposed Adaptive Autoregressive-WWO algorithm, the coefficients of second order polynomial interpolation filter are found. The output generated from this filter is referred as S_2 .

3.3.1 Proposed Adaptive Autoregressive-WWO Algorithm for Finding Coefficients of Second Order Polynomial Interpolation Filter:

For determination of coefficients of second order polynomial interpolation filter, this proposed adaptive autoregressive-WWO algorithm is utilized. WWO [23] and CAViaR [22] are combined to form the proposed adaptive autoregressive-WWO algorithm. This is utilized for finding the coefficients of second order polynomial. This proposed method is very useful as it has high performance in quality improvement. They utilize less data of various color channel for the processing. The solution encoding, fitness function and proposed Autoregressive-WWO algorithm are given in below in detail.

• **Solution Encoding:** The solution encoding represents addressing the optimization problems. Here, proposed adaptive autoregressive-WWO is employed for selecting solution for selection of optimal filter coefficient. The arbitrary value is provided from the solution set, which comprises set of filter coefficients. This solution set acquires optimal filter coefficients, that is utilized for second order polynomial interpolation filter by newly devised fitness function. The size of filter coefficients is expressed as c . Fig.3 shows the determination of optimal filter coefficients from the representation of solution.

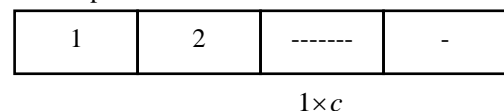


Fig.3. Determination of optimal filter coefficients from the representation of solution

• **Fitness Function:** SDME is the evaluation metric which is used to formulate the fitness of each solution from the

population. The second order measure is found by SDME for solving optimization issue, which is denoted as,

$$SDME = -\frac{1}{d_1 d_2} \sum_{e=1}^{d_1} \sum_{f=1}^{d_2} 20 \ln \left| \frac{Y_{\max}^{e,f} - 2Y_{cen}^{e,f} + Y_{\min}^{e,f}}{Y_{\max}^{e,f} + 2Y_{cen}^{e,f} + Y_{\min}^{e,f}} \right| \quad (7)$$

where, $Y_{\max}^{e,f}$ indicates maximal pixel value, $Y_{\min}^{e,f}$ shows minimal pixel value, and $Y_{cen}^{e,f}$ signifies center pixel value, and also d_1 and d_2 are the image blocks.

3.4 PROPOSED ADAPTIVE AUTOREGRESSIVE-WWO ALGORITHM

The optimal filter coefficients are obtained using proposed Autoregressive-WWO, which is designed by combining WWO [19] and CaViaR [18] model. Here, WWO is motivated from the shallow water wave theory. The algorithm helps to enhance the diversity and minimize premature convergence. The algorithm is feasible and effective in solving real-world issues. The method utilizes breaking operator for enabling intensive search around emerging areas. In addition, the algorithm is effectual in providing good balance amongst exploitation and exploration. The CAViaR model indicates the evolution of quantile with respect to time considering an autoregressive procedure and evaluates the attributes with respect to regression quantiles. It is a statistical method, which is utilized to compute the quantity of potential loss that could occur over a particular time using past records. The proposed Autoregressive-WWO algorithm considers the advantages of both the algorithm that is WWO and CaViaR, thus providing the best solution with improved convergence speed. The detailed explanation of the algorithmic steps of proposed Autoregressive-WWO algorithm is:

Step 1) Initialization: Initially, the image dataset is considered as R with a number of input images. This is formulated as,

$$R = \{R_1, R_2, \dots, R_l, \dots, R_a\}; 1 \leq l \leq a \quad (8)$$

where, a is total number of solutions and l^{th} solution is denoted by R_l .

Step 2) Fitness Evaluation: Eq.(7) is used for the evaluation of fitness. Various iterations are conducted for maximal value to determine the optimal solution.

Step 3) Determination of update position: The final update equation obtained from Autoregressive-WWO algorithm is represented as,

$$R_y' = \mu_0 + \mu_1 F_{d-1} + \mu_2 F_{d-2} + \mu_1 c(F_{d-1}) + \mu_2 c(F_{d-2}) + \text{rand}(-1,1) \beta A_y \quad (9)$$

$$\beta = \beta \delta^{(-c(F) - c_{\min} + \gamma) / (c_{\max} - c_{\min} + \gamma)} \quad (10)$$

In the above equations, γ is made adaptive and it is represented as,

$$\gamma = \frac{1}{P} \left[h - \frac{P}{k_{\max}} \right] \quad (11)$$

where, $c[F_{d-1}]$ is the time $d-1$ quantile and $c[F_{d-2}]$ indicate time $d-2$ quantile, P is maximum iteration, h

is current iteration, p is the balance parameter (0-1) and k_{\max} is the wave height (set k_{\max} as 5 or 6).

Step 4) Re-Evaluation of New Solution using Objective Function: For the new set of solutions, the fitness is again computed for checking the feasibility of the solution. When the replacement is possible, then the solution is updated else it remains the same.

Step 5) Termination: Maximum iteration is repeated till the best solution is obtained. The pseudocode for the proposed Adaptive Autoregressive-WWO is indicated in Table.1. The output thus denoted as S_2 .

Pseudocode of proposed Adaptive Autoregressive-WWO

```

Input: Population  $F$ 
Output: Best solution  $F^*$ 
Begin
Arbitrarily initialize  $n$  waves population;
While stopping criterion is not satisfied do
For each  $o \in F$  do
Propagate  $o$  to new  $o'$  using Eq.(32)
If  $f(o') > f(o)$  then
    If  $f(o') > f(o^*)$  then
        Break  $o'$ ;
        Update  $o^*$  with  $o'$ ;
        Replace  $o^*$  with  $o'$ ;
    Else
        Reduce  $o$  by one;
        Update wavelength;
    End if
End if
End for
Re-evaluate fitness using Eq.(27)
Return  $F^*$ 
End while
End
    
```

3.5 FUSION USING ENTROPY

After that, the fusion process is carried on where the output of DCNN, that is denoted by S_1 and output of proposed Adaptive Autoregressive-WWO that is expressed as S_2 are fused to determine the average value based on entropy, and the equation is expressed as,

$$\text{Avg}(Z) = \frac{1}{2} (S_1 + S_2) \quad (12)$$

where,

$$\text{Fusion} = \begin{cases} Z & ; \text{If Entropy}(Z) = \text{Threshold}(P) \\ S_1 & ; \text{If Entropy}(Z) < P \\ S_2 & ; \text{If Entropy}(Z) > P \end{cases} \quad (13)$$

$$\text{Entropy} = -B \log(B) \quad (14)$$

where, B determines the probability distribution of pixels in an image. Thus, the demosaiced image is formed which is the output image.

4. RESULTS AND DISCUSSION

The proficiency of Adaptive Autoregressive-WWO+LPA-ICI + DCNN with priorly devised model considering two databases in terms of PSNR and SDME is examined. The assessment is performed by changing the noise density.

4.1 EXPERIMENTAL SETUP

The analysis of Adaptive Autoregressive-WWO+LPA-ICI + DCNN is carried out in Matlab considering PC with Windows 10 OS, 2GB RAM, and Intel i3 core processor.

4.2 DATASET DESCRIPTION

The assessment of model is done with two databases, namely Multispectral Image Database and standard image dataset.

4.2.1 Multispectral Image Database: Stuff:

This Multispectral Image Database [20] contains zip file, which includes complete spectral resolution reflectance data that comprises 400nm to 700 nm steps. Each band are accumulated with a 16-bit grayscale PNG image. The names of file considering each image are in format 'object_ms_01.png', wherein 01 indicates first image, and is accumulated at 400nm. Also 02 is accumulated at 410 nm and 31 for 700 nm. The color images are revealed as sRGB values.

4.2.2 Standard Image Dataset:

The standard image dataset represents intrinsic images generated through Matlab. It refers to an array of images in which one can execute assessment by specific functions. The images are utilized through the MATLAB image processing toolbox.

4.3 EXPERIMENTAL OUTCOMES

The experimental outcomes of Adaptive Autoregressive-WWO+LPA-ICI + DCNN are obtained with standard image dataset and Multispectral Image Database.

4.3.1 Using Multispectral Image Database:

The experimental outcomes produced from Multispectral Image Database are depicted in Fig.4. The assessment is carried out in presence of Gaussian noise. In Fig.4(a), the input images accumulated is exposed. In Fig.4(b), the mosaic data generated with provided input image is exposed. In Fig.4(c), the Demosaic data generated from the provided input image is exposed.

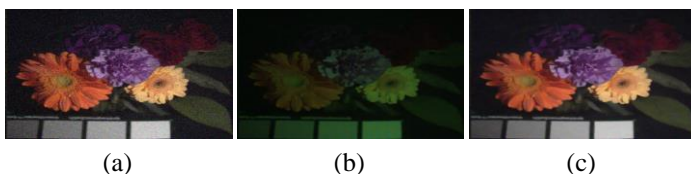


Fig.4. Experimental outcomes with Multispectral Image Database using Gaussian image considering a) Input images b) Mosaic data c) Demosaic data

4.3.2 Using standard dataset:

The experimental outcomes generated from standard dataset are displayed in Fig.4. The assessment is carried out in presence of Gaussian noise. In Fig.4(a), the input images obtained from standard dataset is revealed. In Fig.4(b), the mosaic data generated with provided input image is revealed. In Fig.4(c), the Demosaic data generated from the provided input image is revealed.

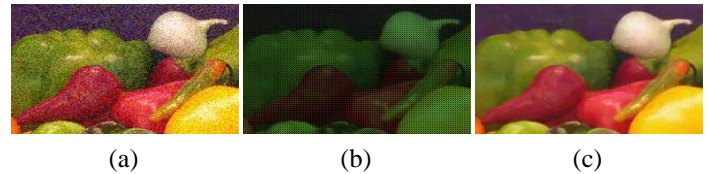


Fig.5. Experimental outcomes with standard dataset considering a) Input images b) Mosaic data c) Demosaic data

4.4 EVALUATION MEASURES

The metrics employed to examine the method includes PSNR, and SDME and is briefly elaborated below.

PSNR: It refers a metric of power to solve noise sleaze in image concerning the Mean Square Error (MSE), and is formulated by,

$$PSNR = 10 \log_{10} \left(\frac{G_{\max}^2}{MSE} \right) \quad (15)$$

where, G_{\max} denote highest image pixel value.

SDME: It is already described in Eq.(7).

4.5 COMPARATIVE METHODOLOGIES

The methodologies employed for analysis includes: RBF [13], IRI [14], CNN [15], Adaptive LPA-ICI [16], Autoregressive-WWO+LPA-ICI + DCNN, and proposed Adaptive Autoregressive-WWO+LPA-ICI + DCNN.

4.6 COMPARATIVE ASSESSMENT

The analysis of Adaptive Autoregressive-WWO+LPA-ICI + DCNN with priorly devised models is performed using PSNR and SDME.

4.6.1 Analysis with Standard Image Dataset:

The assessment in terms of PSNR and SDME with standard image dataset considering Gaussian noise and salt-pepper noise is illustrated.

• Assessment with Salt and Pepper Noise

The Fig.6 presents the assessment with standard image dataset using salt and pepper noise. The PSNR assessment graph is exposed in Fig.6(a). For noise density=0.05, the PSNR calculated by RBF, IRI, CNN, Adaptive LPA-ICI, Autoregressive-WWO+LPA-ICI + DCNN, and Adaptive Autoregressive-WWO+LPA-ICI + DCNN are 31.955dB, 35.901dB, 37.494dB, 38.853dB, 42.557dB, and 42.876dB. Also, for noise density=0.09, the PSNR calculated by RBF, IRI, CNN, Adaptive LPA-ICI, Autoregressive-WWO+LPA-ICI + DCNN, and Adaptive Autoregressive-WWO+LPA-ICI + DCNN are 31.364dB, 34.738dB, 36.247dB, 37.292dB, 40.049dB, and

40.379dB. The proficiency of existing in contrast to proposed Adaptive Autoregressive-WWO+LPA-ICI + DCNN using PSNR are 22.325%, 13.970%, 10.233%, 7.645%, 0.817%. The SDME assessment graph is exposed in Fig.6(b). For noise density=0.05, the SDME calculated by RBF, IRI, CNN, Adaptive LPA-ICI, Autoregressive-WWO+LPA-ICI + DCNN, and Adaptive Autoregressive-WWO+LPA-ICI + DCNN are 40.737dB, 43.984dB, 44.716dB, 47.957dB, 51.442dB, and 51.786dB. Also, for noise density=0.09, the SDME calculated by RBF, IRI, CNN, Adaptive LPA-ICI, Autoregressive-WWO+LPA-ICI + DCNN, and Adaptive Autoregressive-WWO+LPA-ICI + DCNN are 39.509dB, 42.238dB, 43.174dB, 46.502dB, 50.168dB, and 50.675dB. The proficiency of existing in contrast to proposed Adaptive Autoregressive-WWO+LPA-ICI + DCNN using SDME are 22.034%, 16.649%, 14.802%, 8.234%, 1%.

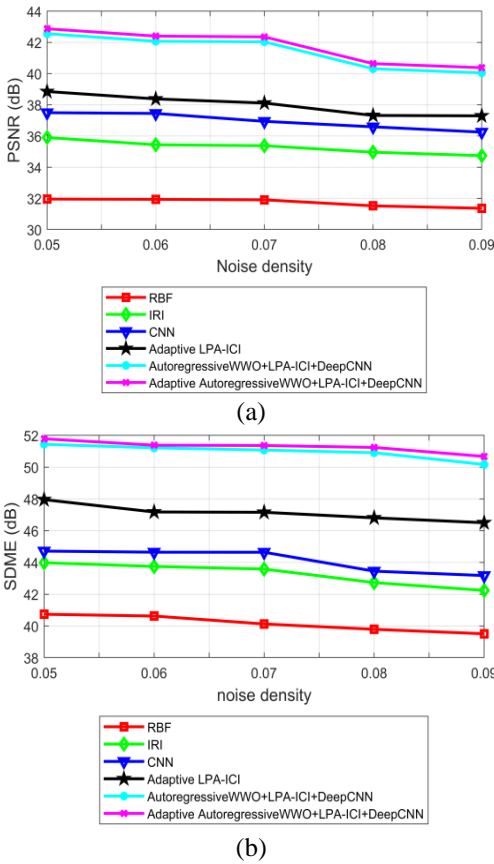


Fig.6. Assessment with standard image dataset using salt and pepper noise considering a) PSNR b) SDME

• **Assessment with Gaussian Noise**

The assessment with standard image dataset using Gaussian noise is exposed in Fig.7. The PSNR analysis graph is revealed in Fig.7(a). When noise density is 0.05, the PSNR calculated by RBF, IRI, CNN, Adaptive LPA-ICI, Autoregressive-WWO+LPA-ICI + DCNN are 22.227dB, 24.235dB, 26.534dB, 32.587dB, 37.993dB, whereas Adaptive Autoregressive-WWO+LPA-ICI + DCNN is 38.587dB. Also, when noise density is 0.09, the PSNR calculated by RBF, IRI, CNN, Adaptive LPA-ICI, Autoregressive-WWO+LPA-ICI + DCNN are 21.277dB, 23.283dB, 25.008dB, 31.614dB, 36.143dB, whereas Adaptive Autoregressive-WWO+LPA-ICI + DCNN is 37.457dB. The proficiency of existing in contrast to proposed Adaptive

Autoregressive-WWO+LPA-ICI + DCNN using PSNR are 43.196%, 37.840%, 33.235%, 15.599%, 3.508%. The SDME assessment graph is exposed in Fig.7(b). When noise density is 0.05, the SDME calculated by RBF, IRI, CNN, Adaptive LPA-ICI, Autoregressive-WWO+LPA-ICI + DCNN are 32.429dB, 35.412dB, 37.729dB, 39.402dB, 49.365dB, whereas Adaptive Autoregressive-WWO+LPA-ICI + DCNN is 49.786dB. Also, for noise density=0.09, the SDME calculated by RBF, IRI, CNN, Adaptive LPA-ICI, Autoregressive-WWO+LPA-ICI + DCNN are 31.267dB, 34.294dB, 36.256dB, 38.809dB, 48.375dB, whereas Adaptive Autoregressive-WWO+LPA-ICI + DCNN is 48.678dB. The proficiency of existing in contrast to proposed Adaptive Autoregressive-WWO+LPA-ICI + DCNN using SDME are 35.767%, 29.549%, 25.518%, 20.274%, 0.622%.

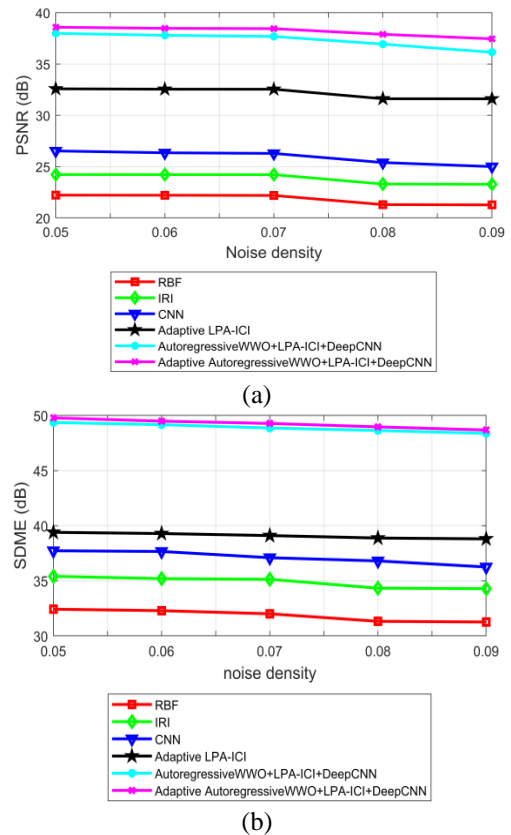


Fig.7. Assessment with standard image dataset using Gaussian noise considering a) PSNR b) SDME

4.6.2 **Analysis considering Multispectral Image Database:**

The assessment in terms of PSNR and SDME with Multispectral Image Database considering Gaussian noise and salt-pepper noise is illustrated.

• **Assessment with Salt and Pepper Noise**

The Fig.8 presents the assessment with Multispectral Image Database using salt and pepper noise. The PSNR assessment graph is exposed in Fig.8(a). Considering noise density=0.05, the PSNR calculated by RBF is 34.747dB, IRI is 35.681dB, CNN is 36.853dB, Adaptive LPA-ICI is 38.755dB, Autoregressive-WWO+LPA-ICI + DCNN is 40.490dB, and Adaptive Autoregressive-WWO+LPA-ICI + DCNN is 40.657dB. Also, considering noise density=0.09, the PSNR calculated by RBF is 33.732dB, IRI is 34.690dB, CNN is 35.693dB, Adaptive LPA-ICI

is 37.750dB, Autoregressive-WWO+LPA-ICI + DCNN is 39.358dB, and Adaptive Autoregressive-WWO+LPA-ICI + DCNN is 39.896dB. The proficiency of existing in contrast to proposed Adaptive Autoregressive-WWO+LPA-ICI + DCNN using PSNR are 15.450%, 13.048%, 10.534%, 5.378%, 1.348%. The SDME assessment graph is exposed in Fig.8(b). Considering noise density=0.05, the SDME calculated by RBF is 42.917dB, IRI is 42.378dB, CNN is 48.694dB, Adaptive LPA-ICI is 46.402dB, Autoregressive-WWO+LPA-ICI + DCNN is 50.674dB, and Adaptive Autoregressive-WWO+LPA-ICI + DCNN is 51.047dB. Also, considering noise density=0.09, the SDME calculated by RBF is 41.970dB, IRI is 41.690dB, CNN is 47.883dB, Adaptive LPA-ICI is 45.657dB, Autoregressive-WWO+LPA-ICI + DCNN is 49.007dB, and Adaptive Autoregressive-WWO+LPA-ICI + DCNN is 49.567dB. The proficiency of existing in contrast to proposed Adaptive Autoregressive-WWO+LPA-ICI + DCNN using SDME are 15.326%, 15.891%, 3.397%, 7.888%, 1.129%.

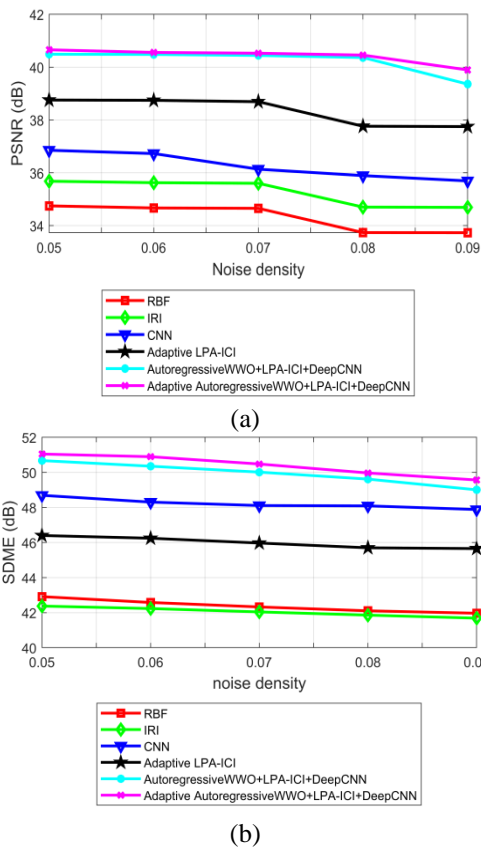


Fig.8. Assessment with Multispectral Image Database using salt and pepper noise considering a) PSNR b) SDME

• **Assessment with Gaussian Noise:**

The assessment with Multispectral Image Database using Gaussian noise is exposed in Fig.9. The PSNR assessment graph is exposed in Fig.9(a). For noise density=0.05, the highest PSNR of 40.343dB is calculated by Adaptive Autoregressive-WWO+LPA-ICI + DCNN while that of RBF, IRI, CNN, Adaptive LPA-ICI, Autoregressive-WWO+LPA-ICI + DCNN are 20.777dB, 23.784dB, 21.460dB, 26.097dB, 39.793dB. Also, for noise density=0.09, the highest PSNR of 40.145dB is calculated by Adaptive Autoregressive-WWO+LPA-ICI + DCNN while that of RBF, IRI, CNN, Adaptive LPA-ICI,

Autoregressive-WWO+LPA-ICI + DCNN are 20.735dB, 23.747dB, 18.112dB, 24.095dB, 39.624dB. The proficiency of existing in contrast to proposed Adaptive Autoregressive-WWO+LPA-ICI + DCNN using PSNR are 48.349%, 40.846%, 54.883%, 39.980%, 1.297%. The SDME assessment graph is exposed in Fig.9(b). For noise density=0.05, the highest SDME of 48.868dB is calculated by Adaptive Autoregressive-WWO+LPA-ICI + DCNN while that of RBF, IRI, CNN, Adaptive LPA-ICI, Autoregressive-WWO+LPA-ICI + DCNN are 29.429dB, 29.412dB, 28.256dB, 39.402dB, 48.365dB. Also, for noise density=0.09, the highest SDME of 47.848dB is calculated by Adaptive Autoregressive-WWO+LPA-ICI + DCNN while that of RBF, IRI, CNN, Adaptive LPA-ICI, Autoregressive-WWO+LPA-ICI + DCNN are 29.012dB, 29.141dB, 27.666dB, 38.809dB, 47.375dB, and. The proficiency of existing in contrast to proposed Adaptive Autoregressive-WWO+LPA-ICI + DCNN using SDME are 39.366%, 39.096%, 42.179%, 18.894%, 0.988%.

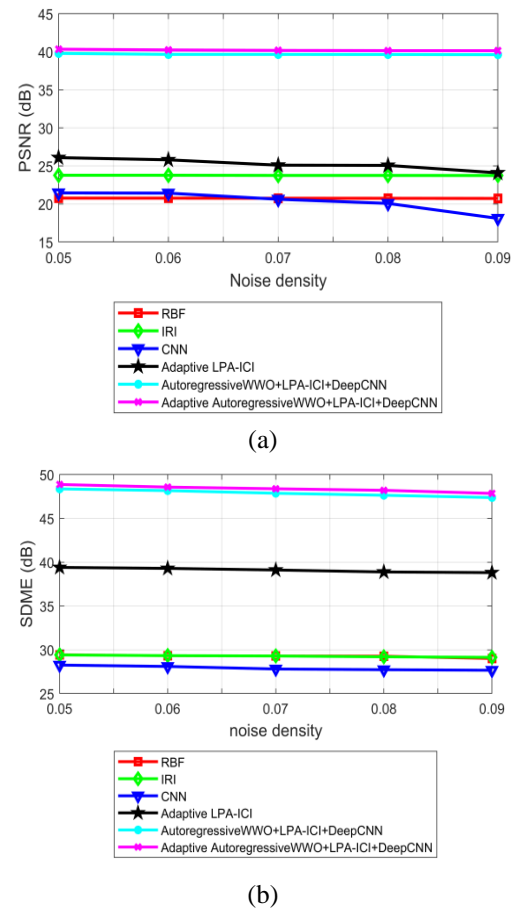


Fig.9. Assessment with Multispectral Image Database using Gaussian noise considering a) PSNR b) SDME

4.7 COMPARATIVE DISCUSSION

The Table.2 displays the assessment with SDME and PSNR using two databases by varying noise density. Using standard image dataset with salt and pepper noise, the highest PSNR of 40.379dB is calculated by Adaptive Autoregressive-WWO+LPA-ICI + DCNN whereas PSNR of RBF, IRI, CNN, Adaptive LPA-ICI, Autoregressive-WWO+LPA-ICI + DCNN are 31.364dB, 34.738dB, 36.247dB, 37.292dB, and 40.049dB.

Table.2. Comparative Assessment

Dataset	Noise type	Metrics	RBF	IRI	CNN	Adaptive LPA-ICI	Autoregressive-WWO+LPA-ICI + DCNN	Proposed Adaptive Autoregressive-WWO+LPA-ICI + DCNN
Standard Image Dataset	Salt and pepper	PSNR (dB)	31.364	34.738	36.247	37.292	40.049	40.379
		SDME (dB)	39.509	42.238	43.174	46.502	50.168	50.675
	Gaussian	PSNR (dB)	21.277	23.283	25.008	31.614	36.143	37.457
		SDME (dB)	31.267	34.294	36.256	38.809	48.375	48.678
Multispectral Image Database	Salt and pepper	PSNR (dB)	33.732	34.690	35.693	37.750	39.358	39.896
		SDME (dB)	41.970	41.690	47.883	45.657	49.007	49.567
	Gaussian	PSNR (dB)	20.735	23.747	18.112	24.095	39.624	40.145
		SDME (dB)	29.012	29.141	27.666	38.809	47.375	47.848

The highest PSNR is due to the proposed model which helps to increase the quality of demosaiced image. With salt and pepper noise, the highest SDME of 50.675dB is calculated by Adaptive Autoregressive-WWO+LPA-ICI + DCNN whereas SDME of RBF, IRI, CNN, Adaptive LPA-ICI, Autoregressive-WWO+LPA-ICI+ DCNN are 39.509dB, 42.238dB, 43.174dB, 46.502dB, and 50.168dB. The highest SDME reveals that the proposed model is effective in determining the coefficients of second order polynomial interpolation filter. With Gaussian noise, the highest PSNR of 37.457dB and highest SDME of 48.678dB are calculated by Adaptive Autoregressive-WWO+LPA-ICI + DCNN. Using Multispectral Image Database with salt and pepper noise, the highest PSNR of 39.896dB and SDME of 49.567dB is calculated by Adaptive Autoregressive-WWO+LPA-ICI + DCNN. With Gaussian noise, the highest PSNR of 40.145dB and SDME of 47.848dB are calculated by Adaptive Autoregressive-WWO+LPA-ICI + DCNN.

5. CONCLUSION

In this paper, DCNN based optimization algorithm for image demosaicing is performed. The main aim of this research is developing an optimization algorithm for the generation of filter coefficients. First, the input image is fed to DCNN that produced the residual output image. Simultaneously, the input image is fed to proposed Adaptive Autoregressive WWO-based LPA-ICI filter for generating filtering coefficients. This proposed Adaptive Autoregressive WWO generated the second-order polynomial interpolation filter coefficients. The developed Adaptive Autoregressive WWO is obtained by combining algorithm and CAViaR model. The residual image outputs generated from the proposed Adaptive Autoregressive WWO-based LPA-ICI filter and DCNN are fused using entropy measure. The fusion of two residual image outputs is utilized for generating the final output, which is the demosaiced image. The proposed Adaptive Autoregressive WWO-based LPA-ICI and DCNN provided better performance with highest PSNR of 40.379dB and highest SDME of 50.675dB. In future, various other measures can be adopted for the fusion process and the feasibility of developed technique can be checked.

REFERENCES

- [1] W. Xing and K. Egiazarian, "Residual Swin Transformer Channel Attention Network for Image Demosaicing", *Proceedings of International Conference Image Processing*, pp. 1-8, 2022.
- [2] C.W. Park and I.K. Eom, "Image Tampering Localization using Demosaicing Patterns and Singular Value Based Prediction Residue", *IEEE Access*, Vol. 9, pp. 91921-91933, 2021.
- [3] M. Pistellato and A. Torsello, "Deep Demosaicing for Polarimetric Filter Array Cameras", *IEEE Transactions on Image Processing*, Vol. 31, pp. 2017-2026, 2022.
- [4] J. Luo and J. Wang, "Image Demosaicing based on Generative Adversarial Network", *Mathematical Problems in Engineering*, Vol. 45, No. 2, pp. 1-14, 2020.
- [5] W. Xing and K. Egiazarian, "End-to-End Learning for Joint Image Demosaicing, Denoising and Super-Resolution", *Proceedings of IEEE Conference on Computer Vision and Pattern Recognition*, pp. 3507-3516, 2021.
- [6] K. Hirakawa and T.W. Parks, "Joint Demosaicing and Denoising", *IEEE Transactions on Image Processing*, Vol. 15, No. 8, pp. 2146-2157, 2006.
- [7] L. Zhang and W. Wu, "Color Demosaicking via Directional Linear Minimum Mean Square-Error Estimation", *IEEE Transactions on Image Processing*, Vol. 14, No. 12, pp. 2167-2178, 2005.
- [8] M. Gharbi and F. Durand, "Deep Joint Demosaicking and Denoising", *ACM Transactions on Graphics*, Vol. 35, No. 6, pp. 1-12, 2016.
- [9] R. Tan and L. Zhang, "Color Image Demosaicking via Deep Residual Learning", *Proceedings of IEEE International Conference on Multimedia and Expo*, pp. 1-13, 2017.
- [10] J.F. Bell, D. Wellington and K. Kinch, "The Mars Science Laboratory Curiosity rover Mastcam Instruments: Preflight and In-Flight Calibration, Validation, and Data Archiving", *Earth and Space Science*, Vol. 4, No. 7, pp. 1-14, 2017.
- [11] P. Getreuer, "Malvar-He-Cutler Linear Image Demosaicking", *Image Processing on Line*, Vol. 1, pp. 83-89, 2011.
- [12] C. Kwan, J.F. Bell and H. Kerner, "Demosaicing Enhancement using Pixel-Level Fusion", *Signal, Image and Video Processing*, Vol. 12, No. 4, pp. 749-756, 2018.

- [13] O.A. Elgendy and J. Ma, "Low-Light Demosaicking and Denoising for Small Pixels using Learned Frequency Selection", *IEEE Transactions on Computational Imaging*, Vol. 7, pp. 137-150, 2021.
- [14] V.N.V. Satya Prakash and T. Jaya Chandra Prasad, "Color Image Demosaicing using Sparse Based Radial Basis Function Network", *Alexandria Engineering Journal*, Vol. 56, No. 4, pp. 477-483, 2017.
- [15] W. Ye, "Color Image Demosaicing using Iterative Residual Interpolation", *IEEE Transactions on Image Processing*, Vol. 24, No. 12, pp. 5879-5891, 2015.
- [16] K. Zhang and L. Zhang, "Learning Deep CNN Denoiser Prior for Image Restoration", *Proceedings of IEEE International Conference on Computer Vision and Pattern Recognition*, pp. 3929-3938, 2017.
- [17] D. Paliy and K. Egiazarian, "Spatially Adaptive Color Filter Array Interpolation for Noiseless and Noisy Data", *International Journal of Imaging Systems and Technology*, Vol. 17, No. 3, pp. 105-122, 2007.
- [18] R.F. Engle and S. Manganelli, "CAViaR: Conditional Autoregressive Value at Risk by Regression Quantiles", *Journal of Business and Economic Statistics*, Vol. 22, No. 4, pp. 367-381, 2004.
- [19] Y.J. Zheng, "Water Wave Optimization: A New Nature-Inspired Metaheuristic", *Computers and Operations Research*, Vol. 55, pp. 1-11, 2015.
- [20] Multispectral Image Database: Stuff, Available at <https://www.cs.columbia.edu/CAVE/databases/multispectral/stuff/>, Accessed in 2022.